JACS
JOURNAL OF THE AMERICAN CHEMICAL SOCIETY

ARTICLE

pubs.acs.org/JACS

Observation of Intermolecular Interactions in Large Protein Complexes by 2D-Double Difference Nuclear Overhauser Enhancement Spectroscopy: Application to the 44 kDa Interferon−Receptor Complex

Ilona Nudelman,[†,§] Sabine R. Akabayov,[†,∥] Tali Scherf,[‡] and Jacob Anglister*[,†]

[†]Department of Structural Biology, and [‡]Chemical Research Support, Weizmann Institute of Science, Rehovot 76100, Israel

Supporting Information

ABSTRACT: NMR detection of intermolecular interactions between protons in large protein complexes is very challenging because it is difficult to distinguish between weak NOEs from intermolecular interactions and the much larger number of strong intramolecular NOEs. This challenging task is exacerbated by the decrease in signal-to-noise ratio in the often used isotope-edited and isotope-filtered experiments as a result of enhanced T_2 relaxation. Here, we calculate a double difference spectrum that shows exclusively intermolecular NOEs and manifests the good signal-to-noise ratio in 2D homonuclear NOESY spectra even for large proteins. The method is straightforward and results in a complete picture of all intermolecular interactions involving non exchangeable protons. Ninety-seven such ^{1}H−^{1}H NOEs were assigned for the 44 KDa interferon−α2/IFNAR2 complex and used for docking these two proteins. The symmetry of the difference spectrum, its superb resolution, and unprecedented signal-to-noise ratio in this large protein/receptor complex suggest that this method is generally applicable to study large biopolymeric complexes.

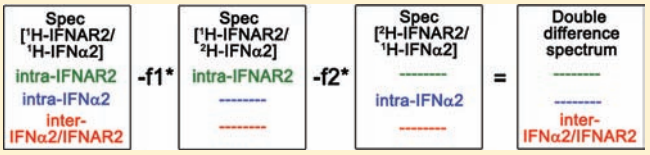

INTRODUCTION

NMR is a powerful technique for the three-dimensional structure determination of proteins in solution. The development of improved heteronuclear experiments and the increased sensitivity of modern NMR spectrometers equipped with cryoprobes have raised the size limit of proteins for which high-resolution structure can be determined to about 45−50 kDa.[1] Low-resolution structures of proteins up to 100 kDa molecular mass have been determined.[2] However, NMR structures of proteins larger than 40 kDa are still scarce.

Structure determination of protein complexes by NMR is even more demanding because of the need to observe and assign a large number of proton−proton interactions between the biomolecules in the complex and to resolve weak intermolecular NOEs from the much larger number of strong intramolecular connectivities. This challenging task is aggravated in large protein complexes because of the decrease in signal-to-noise ratio in heteronuclear experiments due to shorter T_2 relaxation times and the increased overlap in the NMR spectra. As a result, the number of structures obtained for protein complexes by NMR is rather small, and currently there are only 322 NMR structures of protein complexes available in the PDB (out of which only 30 are of protein complexes larger than 40 kDa, most of which did not include any intermolecular NOE data).

One way to overcome the obstacles in identifying intermolecular interactions is to label one of the components of the complex with ^{15}N and/or ^{13}C, while the second component remains unlabeled. Using a combination of isotope filtered-edited experiments, it is possible to identify NOEs across interfaces between two protons, where only one is bonded to a labeled heteroatom.[3−7] However, with increasing size of protein complexes, these experiments become much less sensitive. The use of asymmetrically labeled complexes in which one component is labeled with ^{13}C/^{1}H-Ile, Leu, and Val methyl groups on a background of complete deuteration and the other protein is unlabeled can alleviate the signal-to-noise ratio problem and enable the study of intermolecular interactions involving methyl protons.[8−11] However, this method yields only NOEs involving the methyl groups of Ile, Leu, and Val and in addition requires the use of 3D ^{13}C-edited NOESY spectra, which are inherently less sensitive for high molecular weight systems than for their 2D counterparts.

Homonuclear 2D NOESY spectra exhibit high signal-to-noise ratios even for large proteins because magnetization transfer takes place when the magnetization is in the z-direction, in contrast to all other multidimensional NMR experiments, which involve magnetization transfer in the xy plane. The relaxation of magnetization in the z-direction depends on T_1 and is slow even for large proteins (∼0.5−1 s) in comparison with the T_2 relaxation (in the xy plane) time, which is shorter than 10 ms for proteins with a molecular mass greater than 50 kDa.

Recently, we demonstrated that 2D NOESY spectra in combination with asymmetric reverse-protonation of deuterated proteins can provide detailed information about intermolecular interactions in large protein complexes.[12] To simplify the spectra and extract intermolecular NOEs, one protein in the complex was uniformly deuterated and reverse-protonated with selected aromatic amino acids, while the other protein in the complex was uniformly deuterated and reverse-protonated with selected

Received: June 13, 2011
Published: August 08, 2011

aliphatic amino acids.[12] The high sensitivity of the 2D NOESY spectrum, even for the 44 kDa IFNAR2/IFNα2 complex (IFN - interferon; IFNAR2 - extra-cellular part of the second subunit of the receptor for type 1 interferons) at a concentration of 0.25 mM, enabled the detection of 24 intermolecular NOEs with a high signal-to-noise ratio.[12] The distance constraints obtained on the basis of the assigned intermolecular NOEs led to a considerably improved model of the 44 kDa IFNAR2/IFNα2 complex;[12] however, information was obtained only on a small fraction of intermolecular interactions and was restricted to NOEs between aromatic residues and nonaromatic residues with chemical shifts smaller than 2.2 ppm.

NOESY difference spectra can be used to extract information about the conformation of small tightly bound ligands and their interactions with large proteins.[13−15] We used NOESY difference spectra to study the conformation of an HIV-1 gp120 V3 peptide bound to the 50 kDa Fab fragment of an HIV-1 neutralizing antibody as well as the interactions between them.[16] The difference was between the NOESY spectrum of the unlabeled complex and the NOESY spectrum of the Fab complex with a V3 peptide in which selected residues were deuterated. Assignment of the NOEs observed in the difference spectrum to the specific pairs of antibody−peptide protons was accomplished by a combination of deuteration of either the Fab molecule or V3 residues, Fab chain-specific labeling, and examination of the antibody binding site structure. The assigned NOEs as well as double mutant cycle (DMC) constraints were used to calculate a docking model for the Fab−peptide complex.[16]

Here, we describe a straightforward, powerful method for the detection of intermolecular interactions in large proteins or biopolymeric complexes. This method is based on the sequential subtraction of the 2D NOESY spectra of two different samples in which only one of the complex components is perdeuterated, from the 2D NOESY spectrum of the unlabeled complex. The sequential subtraction cancels out the intramolecular NOEs of each of the two protein components of the complex, and only the intermolecular NOEs remain in the difference spectrum. Our double difference NOESY spectrum approach was applied to the 44 kDa IFNAR2/IFNα2 complex, allowing identification of 97 intermolecular NOEs with excellent signal-to-noise ratio despite the low concentration of the samples (0.25 mM). The high quality of the difference spectrum in regions showing both the aromatic−aliphatic and the aliphatic−aliphatic interactions implies that this method is generally applicable and can be used to obtain an unprecedented detailed and well-resolved picture of intermolecular interactions involving non exchangeable protons even for high molecular weight biopolymeric complexes.

EXPERIMENTAL METHODS

Expression of IFNAR2 and IFNα2. Unlabeled and uniformly deuterated IFNAR2 and IFNα2 were prepared by overexpression in *E. coli* strain Rosetta (DE3) (Novagen) transformed with the plasmid pET27b (Novagen) into which the genes of interest were cloned. Following transformation, the bacterial cells were grown in LB medium for unlabeled proteins and in M9/D_2O minimal media supplemented with 0.1% $^{14}NH_4Cl$ and 0.3% ^{12}C,^{2}H-glucose for uniformly deuterated proteins. Expression was induced by 0.1% IPTG, and cells were grown postinduction for 8 h. Purification of IFNAR2 and IFNα2 was performed following previously published protocols.[17−19]

NMR Sample Preparation. Three NMR samples were prepared: ^{1}H-IFNAR2/^{1}H-IFNα2, U-^{2}H-IFNAR2/^{1}H-IFNα2, and ^{1}H-IFNAR2/U-^{2}H-IFNα2. All complexes were prepared as previously described[12] at a molar IFNAR2:IFNα2 ratio of 1:1. Protein concentrations were ascertained by their molar extinction coefficients calculated from the primary amino acid sequence using the ProtParam tool in the ExPASy Proteomics Server.[20] The extinction coefficients used were 28 795 and 18 700 M^{-1} cm^{-1} for IFNAR2 and IFNα2, respectively. All samples were exchanged to the same D_2O-based buffer (25 mM d_{11}-Tris pD 8, 0.02% NaN3, 99.9% D_2O) by repeated dilution/concentration cycles using Amicon Ultra tubes (Millipore, MW cutoff 10 kDa). The final concentration of the complex in all samples was 0.25 mM.

NMR Measurements. All NMR spectra were acquired at 305 K on a Bruker AVIII 800 MHz spectrometer equipped with a 5 mm Triple-Resonance Inverse TCI CryoProbe with Z-gradients and with an Automatic Tuning and Matching (ATM) unit. Data were processed and analyzed using the NMRDraw/NMRPipe[21] and NMRView[22] software packages.

The 2D NOESY spectra were acquired using 400 t_1 increments and 4096 t_2 points with a sweep width of 11 160.7 Hz in both dimensions. An interscan delay of 2 s was applied. NOESY mixing time was 80 ms for the spectra used for final analysis, assignment, and modeling; however, spectra with mixing times of 40 and 200 ms were also acquired and analyzed (see Supporting Information Figure S1). The decision to use the spectra recorded with 80 ms mixing time was based on the signal-to-noise ratio of cross-peaks versus the strength of subtraction artifacts (see Supporting Information Figure S1). The 200 ms spectrum contained contributions from spin diffusion, whereas the 40 ms spectrum showed much fewer cross-peaks, especially in the aliphatic and the aromatic-Hα/Hβ regions relative to the 80 ms spectrum. This was probably due to the fact that 40 ms mixing time is not sufficient to detect the weak intermolecular NOEs (see Supporting Information Figure S1). Residual water magnetization was suppressed with a presaturation pulse. The initial sampling delay was set to $\tau = 4^*\tau_{90}/\pi + t_1(0)$, where τ_{90} is the duration of the 90° pulse and the $t_1(0)$ is the dwell time increment between successive sampled points in the acquisition dimension. This initial sampling delay was used to enable a constant phase correction in the F1 dimension.[23]

Double Difference Spectrum Calculation. All spectra were processed identically except for minor changes in the F2 phases as required in each of the three individual spectra. No baseline correction was applied in the processing of the original spectra. The double subtraction using the 2D subtraction command of NMRPipe[21] software was performed in a sequential manner; that is, first, a spectrum of one of the deuterated complexes was subtracted from the spectrum of the unlabeled one, and then the third spectrum was subtracted from the result of the first subtraction (Figure 1a; Supporting Information Figures S2, S3, S4).

$$\text{first step}: \text{Spec}[^{1}\text{H-IFNAR2}/^{1}\text{H-IFN}\alpha2] - f1^*\text{Spec}[^{1}\text{H-IFNAR2}/^{2}\text{H-IFN}\alpha2]$$

$$\text{second step}: \text{Spec}[\text{result of first step}] - f2^*\text{Spec}[^{2}\text{H-IFNAR2}/^{1}\text{H-IFN}\alpha2]$$

The appropriate subtraction factors $f1$ and $f2$ were determined independently for each subtraction step using the same procedure. For the determination of the $f1$ subtraction factor, the two NOESY spectra to be subtracted (^{1}H-IFNAR2/^{1}H-IFNα2 and ^{1}H-IFNAR2/^{2}H-IFNα2) were overlaid, and a row (row 920) was selected in which the same cross-peaks appeared in both spectra, designating those cross-peaks as intramolecular ^{1}H-IFNAR2 NOEs, which should be canceled out in the subtraction. This row was from a well-resolved region of the spectrum (in our case, the methyl region) to make sure no intramolecular ^{1}H-IFNα2 or intermolecular contributions are present as well as to enable an accurate estimation of cross-peak intensity (Figure 1b,d; Supporting Information Figure S1). Next, rows 920 from both of the subtracted spectra (^{1}H-IFNAR2/^{1}H-IFNα2 and ^{1}H-IFNAR2/^{2}H-IFNα2) were

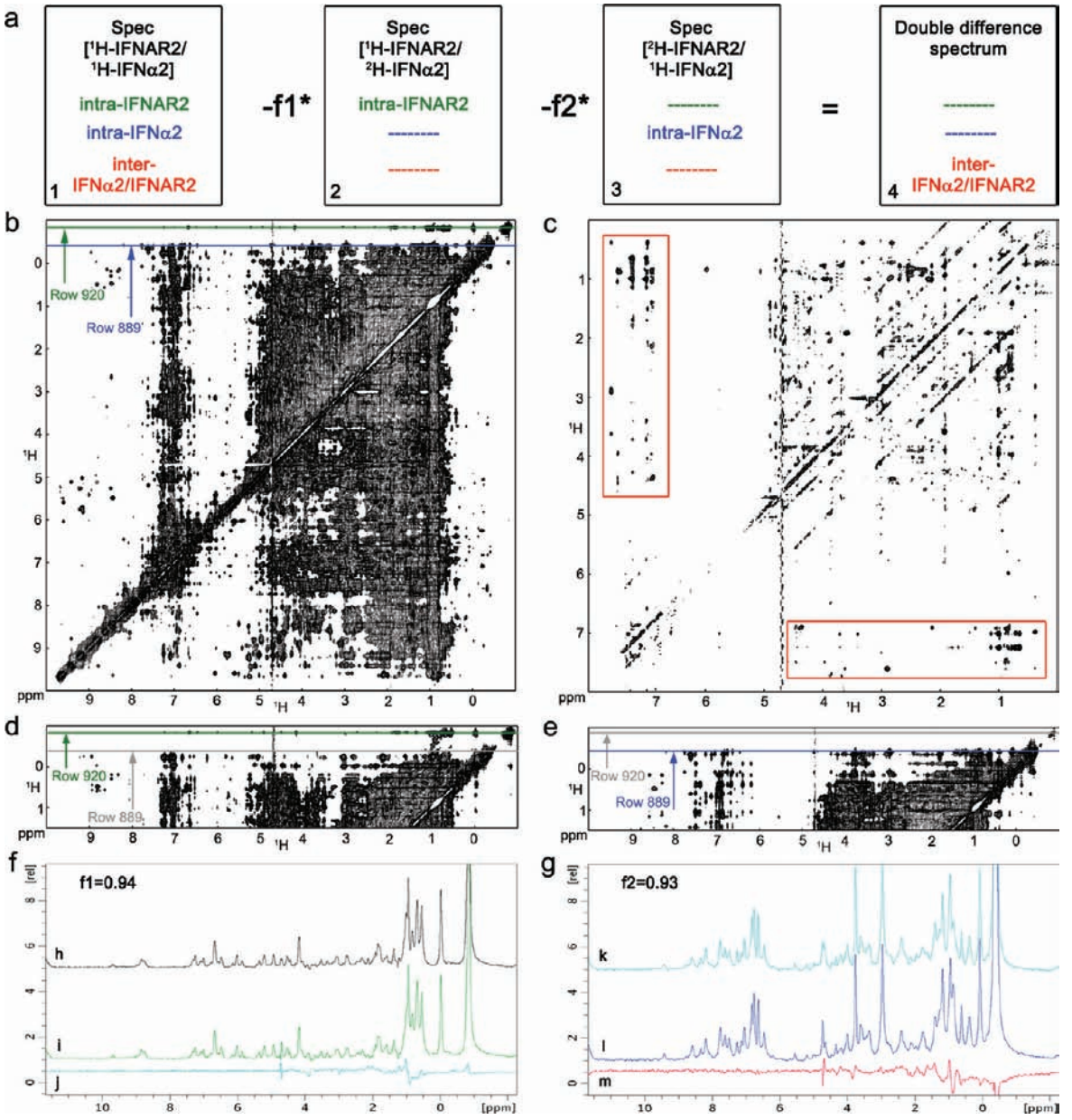

Figure 1. Calculating a double difference NOESY spectrum for the IFNα2/IFNAR2 complex. (a) Schematic representation of subtraction procedure used. Spectral type indicated in black within the boxes (top). Types of interactions: intramolecular interactions in IFNAR2 in green, intramolecular interactions in IFNα2 in blue, and intermolecular interactions indicated in red. *f*1 and *f*2 represent calibration factors needed to obtain nulling of intramolecular connectivities (see Experimental Methods for details). (b) 2D NOESY spectrum of ^{1}H-IFNAR2/^{1}H-IFNα2 showing the rows 920 and 889 used to determine the *f*1 (green) and *f*2 (blue) subtraction factors, respectively. (c) Double difference NOESY spectrum with red boxes showing the symmetry of the obtained difference spectrum in the section of the spectrum showing interactions between aromatic and aliphatic protons (side chains as well as α-protons). (d) Section from the 2D NOESY spectrum of ^{1}H-IFNAR2/^{2}H-IFNα2 showing row 920, which was used to determine the *f*1 factor. Row 889, shown in gray, contains no cross-peaks in this spectrum. (e) Section from the 2D NOESY spectrum of ^{2}H-IFNAR2/^{1}H-IFNα2 showing row 889, which was used to determine the *f*2 factor. Row 920, shown in gray, contains no cross-peaks in this spectrum. (f) 1D projections of row 920 from 2D NOESY spectra of ^{1}H-IFNAR2/^{1}H-IFNα2 (h, black), ^{1}H-IFNAR2/^{2}H-IFNα2 (i, green), and the result of their subtraction using *f*1 = 0.94 (j, light blue). (g) 1D projections of row 889 from 2D NOESY spectra of the result of the first subtraction step: [^{1}H-IFNAR2/^{1}H-IFNα2 − 0.94*^{1}H-IFNAR2/^{2}H-IFNα2] (k, light blue), ^{2}H-IFNAR2/^{1}H-IFNα2 (l, blue), and the result of their subtraction using *f*2 = 0.93 (m, red).

plotted as 1Ds, and the value of the *f*1 subtraction factor was determined according to the intensity ratio between the overlaid cross-peaks (Figure 1f; Supporting Information Figure S3). To ensure the correct factor was chosen, its value was changed to within ±15% of the intensity ratio, and the appearance of the resulting 1D was examined for a subtraction with optimal cancelation of the overlaid cross-peaks. It was found that the intensity ratio was indeed accurate in predicting the appropriate factor for the entire 2D spectrum (see Supporting Information Figures S3, S4). The *f*2 subtraction factor was determined in a similar manner. The values of the subtraction factors found were 0.94 and 0.93 for *f*1 and *f*2, respectively.

A polynomial baseline correction was applied to the double difference spectrum in the F2 dimension to minimize the subtraction artifacts. The final double difference spectrum seemed to require slight adjustment of

dx.doi.org/10.1021/ja205480v |*J. Am. Chem. Soc.* 2011, 133, 14755–14764

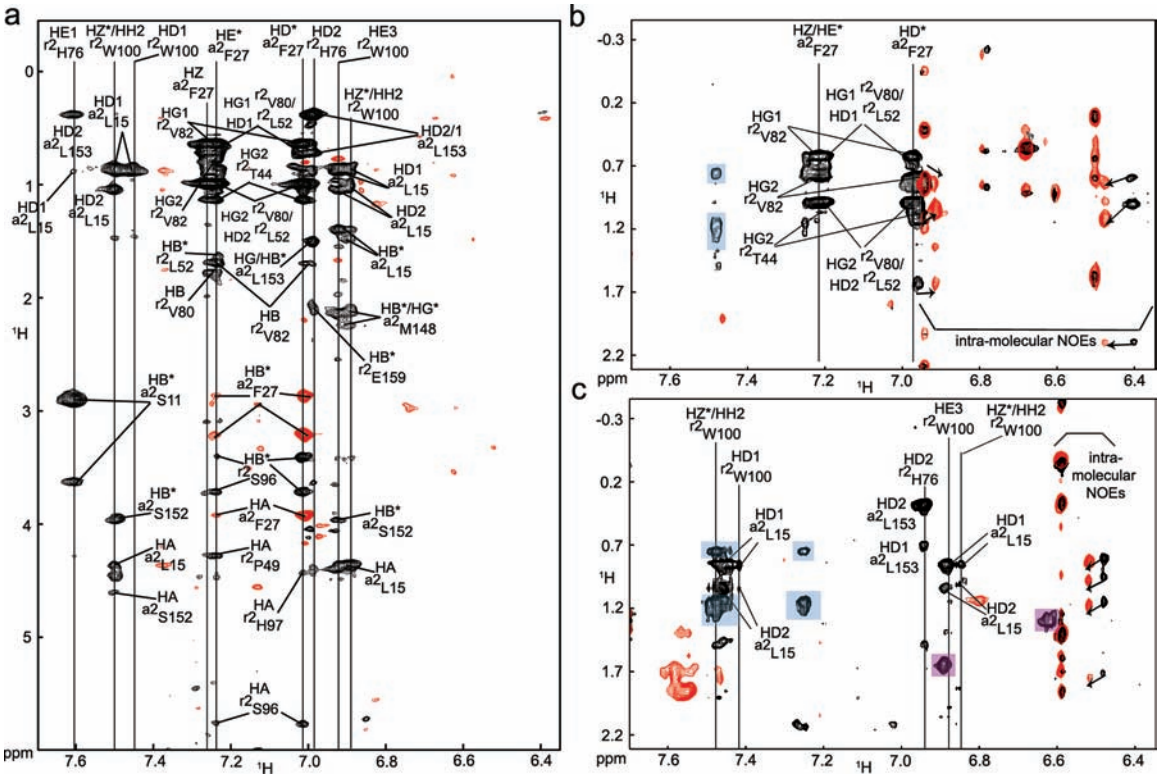

Figure 2. Comparison of the double difference NOESY spectrum (panel a) of the IFNα2/IFNAR2 complex with the spectra obtained by asymmetric labeling (panels b and c). (a) Aromatic region of the double difference NOESY spectrum calculated using the procedure illustrated in Figure 1. Positive cross-peaks are in black, and negative cross-peaks are in red. Vertical lines indicate cross-peaks originating from the same aromatic proton and are labeled at the top of the spectrum according to the assignment of the specific proton. The aliphatic proton assignments are marked for each cross-peak in the spin system. IFNAR2 and IFNα2 residues are labeled with superscripts r2 and a2, respectively. (b) Asymmetric-labeling 2D NOESY spectrum of IFNAR2(HFW)/IFNα2(KRLAM) (black) (the reverse-protonated amino acids are given in parentheses). The NOESY spectrum of free IFNα2-(KRLAM) (red) overlaid on the spectrum of the complex helps to identify intramolecular NOEs in IFNα2(KRLAM) that resulted from incomplete deuteration of this protein.[12] (c) The asymmetric-labeling 2D NOESY spectrum of IFNAR2(IVLTMAK)/IFNα2(HFWY) (black). The NOESY spectrum of free IFNAR2(IVLTMAK) (red)[12] overlaid on the asymmetric-labeling spectrum helps to identify intramolecular NOEs in IFNAR2-(IVLTMAK) that resulted from incomplete deuteration of this protein.[12] Arrows indicate small changes in the positions of the intramolecular cross-peaks between the spectra of the free molecule and the complex. Black cross-peaks not overlaid with red cross-peaks and not marked by arrows originate from intermolecular interactions and are labeled according to the assignment of the aliphatic proton. Vertical lines indicate cross-peaks originating from the same aromatic proton and are labeled at the top of the spectrum according to the assignment of the specific proton. IFNAR2 and IFNα2 residues are labeled with superscripts r2 and a2, respectively. Light blue boxes indicate cross-peaks that appeared after the urea-induced partial denaturation[12] and that are not attributed to intermolecular interactions. Purple boxes indicate the two cross-peaks missing in the double difference spectrum.

the phase in F2. This additional minor phase correction was applied to the original 2D spectra, and the subtraction was carried out again using the predetermined *f*1 and *f*2 subtraction factors.

Docking. The docking of the IFNAR2/IFNα2 complex was performed using the software HADDOCK2.0,[24] which utilizes the crystallography and NMR system (CNS).[25,26] The docking was based on the chemical shift perturbation data for IFNAR2, the cross saturation data for IFNα2, NOE interactions, and mutagenesis data.[17,19,27,28] Starting structures for the docking were the published structures of IFNAR2 (PDB entry 1N6U[27]) and IFNα2 (PDB entry 1ITF[29]). Active and passive residues in IFNα2 and IFNAR2 were selected using the strategy outlined by Dominguez et al.[24] based on the binding sites mapped in previous studies in our group[17,19] and were identical to the ones chosen in the calculation of our previous docking model of the IFNAR2/IFNα2 complex[12] (see Supporting Information Table S1). Following the guidelines of HADDOCK2.0 (http://www.nmr.chem.uu.nl/haddock/), active residues are those identified by experiment (either NMR or mutagenesis experiments) to be involved in the interaction between the two molecules and that have a high solvent accessibility (in our analysis, we have chosen main-chain or side-chain relative accessibility >30%). Passive residues are all solvent-accessible surface neighbors of active residues.[24] Solvent accessibility was calculated using the program NACCESS.[30,31] Additional pair wise distance restraints were defined on the basis of double mutant cycle analysis data found by Roisman et al.,[28] and the full list of unambiguous distance restraints used in the docking calculation is given in Supporting Information Table S1. NOEs with ambiguous assignment were incorporated as floating assignments using CNS format.[25,26] Ambiguous interaction restraints (AIRs) were defined as ambiguous intermolecular distances (d_{iAB}) following the HADDOCK protocol[24] with a maximum upper distance limit of 2 Å between any atom m of an active residue i of protein A (m_{iA}) and any atom n of either an active or a passive residue k (N_{res} in total) of protein B (n_{kB}) (and inversely for protein B).[24] This d_{iAB} value is the program's default, and it can be changed between 2 and 3 Å to enable tight docking of the interacting molecules. The developers of the HADDOCK program provide a detailed logic for the interaction restraint calculations.[24]

A total of 1000 structures were calculated in the rigid body minimization. Semiflexible simulated annealing followed by refinement in explicit water was performed for the best 200 solutions based on the HADDOCK score (weighted sum of all of the energy terms and the

buried surface area). Violation analysis of the final 200 structures showed that all of the unambiguous distance restraints were satisfied for all structures. Solutions were clustered using a 7.5 Å interface rmsd cutoff. 197 out of 200 structures were included in the eight clusters found. Cluster analysis was performed on the four best structures in each cluster to remove the dependency of cluster averages upon their size. The cluster with the lowest average HADDOCK score was considered to be the best solution.

Structure Analysis. The structure of the IFNAR2/IFNα2 complex and the interface were analyzed with PISA (protein interfaces, surfaces, and assemblies service at the European Bioinformatics Institute),[32] MOLMOL (analysis and display of molecules),[33] and the PSVS – Protein Structure Validation Software suite.[34] All molecular pictures were created with Pymol.[35]

We deposited the new docking model in the PDB (2lag). The IFNAR2 and IFNα2 side-chain protons assignments used in this study were previously deposited in the BioMagResBank (BMRB-16677).

RESULTS

Double Difference Spectrum Calculation. 2D NOESY spectroscopy is one of the simplest 2D NMR experiments to run and is among those most widely used for structure determination of macromolecules; however, because of overlap problems, its application is restricted to proteins with molecular weight less than 15 kDa. ^{1}H−^{1}H NOE interactions form the basis for and the most important part of structure determination by NMR. An important additional advantage of the homonuclear NOESY spectrum is its high sensitivity even for high molecular weight proteins. The 2D NOESY spectrum measured for the unlabeled 44 kDa IFNAR2/IFNα2 complex is presented in Figure 1b. No individual NOEs are revealed in the aliphatic (from 1 to 5 ppm) and aromatic (around 7 ppm) regions due to severe overlap. Nevertheless, well-resolved NOE cross-peaks with good signal-to-noise ratios are seen at the edges of the spectrum (Figure 1b and f, upper trace). Thus, the information content for intermolecular contacts contained in the spectrum is high but is not decipherable due to the presence of a large number of intramolecular NOEs that result in the severe overlap in the aliphatic and aromatic regions.

The asymmetric labeling technique that we developed previously, although very powerful in detecting intermolecular interactions between aromatic protons and a select group of nonaromatic protons, suffers from several drawbacks.[12] If the protein complex exhibits slowly exchanging amide protons, as in the case of the IFNα2/IFNAR2 complex, the use of partial denaturation and subsequent refolding in a D_2O-based buffer is necessary to eliminate the signal of these amide protons from the spectra. This treatment risks modification of the ε-amino groups of lysine residues in the denatured protein as seen in our earlier investigation.[12] Performing the partial denaturation in guanidium hydrochloride rather than in urea could potentially resolve this problem.

Moreover, some intramolecular interactions were observed in the aromatic−aliphatic regions of the spectra of the asymmetrically labeled samples between residual protons on the otherwise deuterated aromatic side chains and unlabeled aliphatic amino acids such as leucine, which were added to the deuterated medium as part of the asymmetric labeling procedure (red cross-peaks in Figure 2b and c). These NOEs originated from the small percentage of residual protons in the growth medium, which was 97% deuterated.[12] These residual protons are not expected to contribute any significant artifacts in the double difference spectra because in the absence of the unlabeled amino acids that were intentionally added in the asymmetric labeling protocol, the probability of observing intramolecular NOEs involving only residual protons is very small. Finally, only a subsection of the NOESY spectrum (6−7.8 in the F2 dimension and −1 to 2.2 ppm in the F1 dimension) can be analyzed in the asymmetric labeling technique. For chemical shifts larger than 2.2 ppm, the spectrum suffers from contributions of intraresidue interactions between the aromatic protons and the α- and β-protons of the same residue. In view of these difficulties and limitations, we sought to develop a general and easily applied method that will enable detection of practically all intermolecular interactions involving nonexchangeable protons in large macromolecular complexes.

A NOESY spectrum of a heterodimeric complex is composed of cross-peaks due to intramolecular interactions within each of its components as well as cross-peaks due to intermolecular interactions (Figure 1a, box 1). If one of the proteins in the complex is deuterated and the other is unlabeled, the NOESY spectrum of the complex contains only cross-peaks due to intramolecular interactions within the unlabeled component (Figure 1a, box 2 and box 3). Cross-peaks due to intermolecular interactions are missing in the two spectra in which one of the proteins is deuterated. When both of these NOESY spectra are subtracted from the NOESY spectrum of the unlabeled complex using standard NMR software (see Experimental Methods), only cross-peaks due to intermolecular interactions remain (Figure 1a, box 4). Such a double difference spectrum is seen in Figure 1c. In contrast to the spectrum measured on the complex directly (Figure 1b), the double difference spectrum shows numerous discrete cross-peaks throughout the chemical shift range. Thus, this method reveals the intermolecular connectivities that are essential to calculate the structure of the protein−protein interface.

The complete details of the subtraction procedure are given in the Experimental Methods. Briefly, the three samples must all be prepared at the same concentration and solvent composition. The empirical multiplication factors $f1$ and $f2$, used in the subtraction, must be calibrated by choosing two rows in the unlabeled complex spectrum, one that contains only intramolecular cross-peaks peaks of IFNAR2 and the other that contains only intramolecular cross-peaks of IFNα2. These rows are then compared to the matching rows from the spectra of the complex in which one of the proteins is deuterated and the factors $f1$ and $f2$, which will null the intramolecular cross-peaks, are adjusted empirically by using the "1D subtract" command of the processing software. As can be seen in Figure 1f and g, excellent elimination of intramolecular cross-peaks can be achieved.

The spectra were measured on samples in D_2O and not H_2O, because the amide deuterons will exchange with protons in H_2O and the subtraction will not provide any additional information about amide proton interactions, and measurements in H_2O will make the subtraction more difficult. Moreover, the commonly used pulses for water suppression, such as WATERGATE, result in considerable loss of protons signal in large proteins with short T_2 relaxation times as well as attenuation of resonances close to the water resonance in the acquisition dimension.

Application of all of the measures mentioned above resulted in multiplication factors very close to 1 ($f1 = 0.94$; $f2 = 0.93$), the correction factor for an ideal set of spectra, demonstrating that nearly ideal conditions were obtained. The calculated difference spectrum (Figure 1c) is very well resolved and is symmetrical across the diagonal, testifying to its quality.

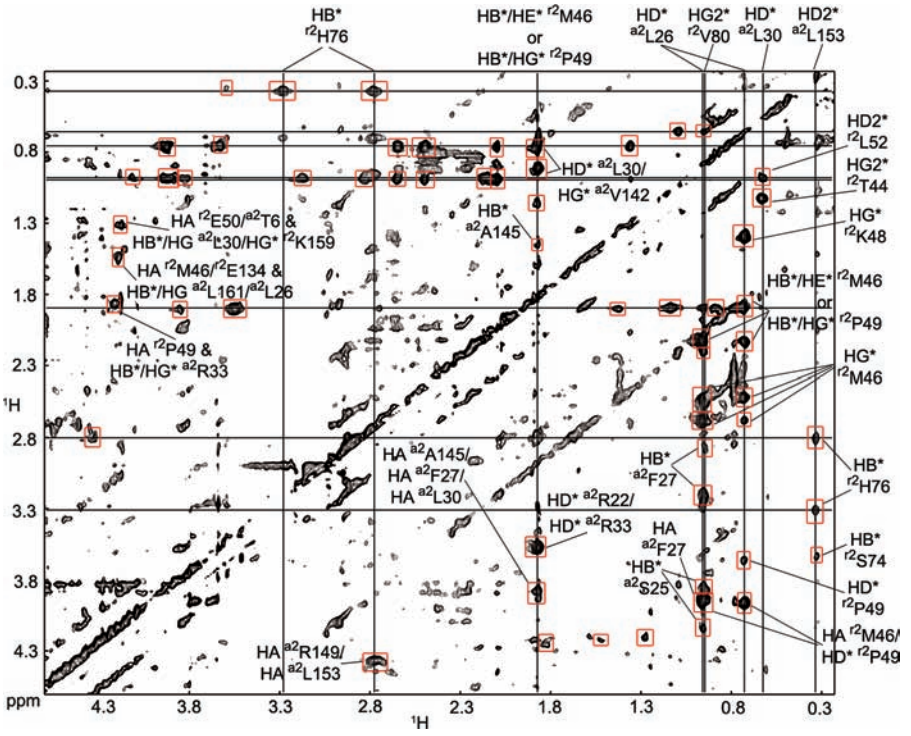

Figure 3. The aliphatic region of the double difference NOESY spectrum of the IFNα2/IFNAR2 complex. Red boxes mark symmetrical cross-peaks, which were designated as intermolecular NOEs. Vertical and horizontal lines indicate cross-peaks originating from the same proton and are labeled according to the assignment of the specific proton. The assignment of the second proton in the interaction is marked for each cross-peak in the spin system. IFNAR2 and IFNα2 residues are labeled with superscripts r2 and a2, respectively. Assignment is presented only for one of the two symmetrical cross peaks.

Intermolecular Interactions between Aromatic and Nonaromatic Protons. To validate the double difference spectrum and make sure that it is free of subtraction artifacts, we compared it to the spectra of the IFNα2/IFNAR2 complex that we previously measured using asymmetric reverse-protonation of IFNα2 and IFNAR2 (Figure 2).[12] To observe intermolecular interactions using the asymmetric reverse-protonation technique, we prepared two IFNAR2/IFNα2 complexes.[12] In the first complex, IFNAR2 was uniformly deuterated and reverse-protonated with the unlabeled aliphatic amino acids isoleucine, valine, leucine, threonine, methionine, alanine, and lysine (IFNAR2(IVLTMAK)), while IFNα2 was uniformly deuterated and reverse-protonated with the unlabeled aromatic amino acids histidine, phenylalanine, tryptophane, and tyrosine (IFNα2(HFWY)).[12] In the second complex, IFNAR2 was reverse-protonated with the aromatic amino acids histidine, phenylalanine, and tryptophan (IFNAR2(HFW)), and IFNα2 was reverse-protonated with lysine, arginine, leucine, alanine, and methionine (IFNα2(KRLAM)).[12] The red cross-peaks and those highlighted in light blue in the asymmetric-labeling spectra presented in Figure 2b and c arise from incomplete deuteration and the urea unfolding/refolding treatment (see above). Therefore, in making our comparison, only the cross-peaks attributed to real intermolecular interactions in the spectra presented in Figure 2b and c were compared to the double difference spectrum (Figure 1a), which is completely free of such artifacts.

As shown in Figure 2, all of the intermolecular interactions that appeared in the asymmetric labeling spectra upfield of 2.2 ppm in the F1 dimension (nonhighlighted black cross-peaks not overlapping with red cross-peaks in Figure 2b,c) were observed also in the double difference spectrum. The only exceptions are two cross-peaks previously assigned to Hγ and Hδ of $^{\alpha 2}$R12 (^{R2}X and $^{\alpha 2}$Y represent IFNAR2 and IFNα2 residues labeled by R2 and α2 superscripts, respectively) (Figure 2c, highlighted in purple).[12] The absence of these two strong cross-peaks in the double difference spectrum implies that they do not correspond to intermolecular interactions but rather could be attributed to intramolecular NOEs involving Hβ protons of one of the aromatic residues of IFNAR2(HFW) with an unusually upfield shifted chemical shift or to amide protons that resisted deuterium-exchange despite the partial unfolding.

The aromatic−aliphatic region of the double difference spectrum revealed several cross-peaks between 1.2 and 2.2 ppm (in F1) that did not appear in the asymmetric labeling spectra. In addition, a spin system assigned to HE1 of ^{r2}H76 (F2 = 7.61 ppm) did not appear in the asymmetric labeling spectra probably due to deuterium exchange of this histidine proton caused by the prolonged incubation of the samples in D_2O[36] during the partial denaturation required to eliminate the cross-peaks of the amide protons in this experiment. In addition to the elimination of artifacts, the spectrum presented in Figure 2a shows at least 15 intermolecular NOEs between aromatic protons and nonaromatic protons with chemical shifts higher than 2.2 ppm. These cross-peaks could not be identified in the asymmetric-labeling spectra because of overlap with the numerous cross peaks resulting from the intraresidue interactions of the aromatic-Hα/Hβ protons.

Although only positive cross-peaks are expected to appear in the double difference spectrum, several negative cross-peaks were observed (red cross-peaks in Figure 2a). These cross-peaks appeared due to strong intraresidue interactions within $^{\alpha 2}$F27 and are not a result of subtraction artifacts or improper choice of

Table 1. List of Intermolecular Distance Restraints Obtained from the Double Difference Spectrum[a]

	IFNα2	IFNAR2
aromatic−aliphatic region	F27:HZ;HE*;HD*	V80:HG1*;HG2*; L52:HD1*;HD2*; V82:HG1*;HG2*; T44:HG2*
	L15:HD1*, HD2*	W100: HZ3/HZ2/HH2;HD1;HE3
	L153:HD1*, HD2*	H76:HD2
	L15:HD1*;	H76:HE1
	L153:HD1*, HD2*	
aromatic−HB/HA region	F27:HD*	V82:HB; S96:HB*;HA; H97:HA
	F27:HE*	L52:HB*;V80:HB; V82:HB; S96:HB*;HA
	F27:HZ	V80:HB; V82:HB; S96:HB*
	L15:HB*;HA;	W100:HZ1/HZ2/HH2
	S152:HB*;HA;	
	M148:HB*/HE*	
	L15:HB*;HA;	W100:HE3
	S152:HB*;	
	M148:HB*/HE*	
	L153:HB*/HG;	H76:HD2
	E159:HB*	
	S11:HB*	H76:HE1
aliphatic region	F27:HB*	S96:HA
	L153:HD2*	H76:HB*; S74:HB*
	L30:HD1*/HD2*	L52:HD2*; T44:HG2*
	L26:HD1*; HD2*	K48:HG*; M46:HB*/HE* or P49:HB*/HG*; M46: HG*; P49:HD*; M46:HA or P49:HD*
	F27:HB*; HA; S25:HB*	V80:HG2*
	L30:HD* or V142:HG*;	M46:HB*/HE* or P49:HB*/HG*
	V142:HG*; A145:HB*;	
	R22:HD* or R33:HD*;	
	F27:HA or L30:HA or A145:HA	
	L153:HA or R149:HA	H76:HB*
	L30:HB*/ HG or T6:HA	E50:HA or K159:HG*
	R33:HB*/HG*	P49:HA
	L161:HB*/HG or L26: HB*/HG	M46:HA or E134:HA

[a] Asterisks stand for ambiguous stereospecific assignment. Colons stand for "and". Slashes stand for "or".

the factors used in the subtraction. $^{\alpha 2}$F27 is protruding out of the IFNα2 surface and is buried in a deep IFNAR2 pocket.[12] Therefore, the relaxation of $^{\alpha 2}$F27 is influenced by IFNAR2 protons. When IFNAR2 is deuterated, the relaxation pathways available to $^{\alpha 2}$F27 decrease and the intraresidue NOEs in $^{\alpha 2}$F27 become stronger than the corresponding cross-peaks in the unlabeled complex. Accordingly, the difference spectrum will contain negative contributions from $^{\alpha 2}$F27 protons. Similarly, other residues at the interface interacting extensively with residues of the partner protein may also exhibit negative intraresidue NOEs in the difference spectrum. Rather than being a drawback, we believe that these negative cross-peaks highlight residues in one protein that are buried in deep pockets in the other protein and thus provide further structural insight about the binding interface.

Intermolecular Interactions between Nonaromatic Protons. The most crowded region of the double difference 2D NOESY spectrum is the section showing interactions between nonexchangeable nonaromatic protons (Figures 1c and 3). The asymmetric labeling technique is restricted to the observation of intermolecular interactions between aromatic amino acids and a select group of aliphatic amino acids consisting of protons resonating upfield of 2.2 ppm (chemical shift smaller than 2.2 ppm). The double difference spectrum provides us with information regarding all intermolecular interactions in the complex: aromatic−aliphatic, aliphatic−aliphatic, and aromatic−aromatic in the entire chemical-shift range (−2 to 8 ppm). This is evidenced by the identification and assignment of 97 intermolecular NOEs in the double difference spectrum in comparison with only 24 NOEs observed by the asymmetric labeling method.

Methyl protons of protein residues, especially those centered around 1 ppm, give the strongest signal in the NMR spectrum. These methyl protons exhibit intense and frequently sharp resonances in comparison with other protein protons due to their increased mobility and high intensity, which may cause subtraction artifacts due to truncation and T_1-noise. Despite these concerns, the aliphatic section of the double difference spectrum of the IFNα2/IFNAR complex is very well resolved, symmetrical, and free of T_1-noise (Figure 3).

Minor artifacts appearing as lines of cross peaks parallel to the diagonal do appear in the difference spectrum (Figure 3). Such artifacts are typical of a periodic instability in the electronics of the controller of the air-conditioning system in the spectrometer room. (Previously, we suffered from very severe parallels to the diagonal artifacts. Most of this problem was resolved by turning off the central air-conditioning system and using wall air-conditioners.) Regardless of the cause, these residual artifacts do not prevent the analysis of the spectrum and the observation

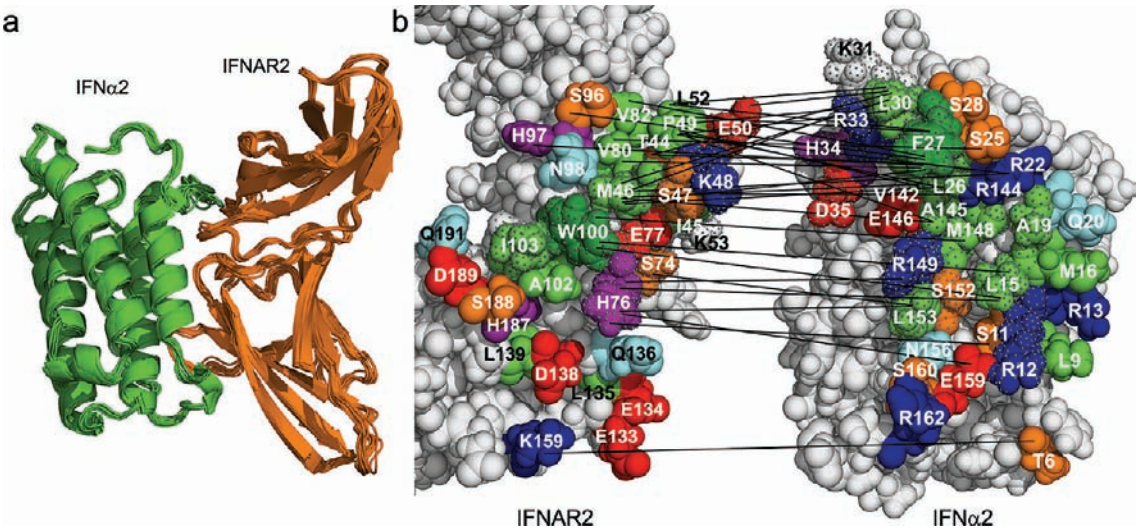

Figure 4. A docking model of IFNAR2/IFNα2 based on intermolecular NOEs obtained from the double difference spectrum. (a) Ensemble of best 10 structures from the highest ranking cluster in the calculation. IFNAR2 is shown in orange, and IFNα2 is in green. The flexible N-terminal (^{R2}S1−^{R2}C12) and C-terminal residues (^{R2}P204− ^{R2}S212) of IFNAR2 were removed for the presentation. (b) Open book representation of the IFNAR2/IFNα2 complex and the observed NOE interactions. IFNAR2 (left) and IFNα2 (right) are presented in a space-fill mode. Interface residues (colored) correspond to a minimal set determined by PISA[32] and MOLMOL[33] with an intermolecular distance criterion ≤4 Å and are shown if present in at least 5 structures out of the 10 structures in the ensemble. Residues are colored as follows: light green, aliphatic; dark green, aromatic; red, negatively charged; blue, positively charged; cyan, N and Q; indigo, H; orange, S and T. Residues marked with dots were found by mutagenesis studies to be important for binding. Residues giving rise to the intermolecular NOEs in the double difference spectrum are connected by black lines.

of most of the intermolecular NOEs because all cross-peaks due to protein−protein interactions were identified based on their symmetry with respect to the diagonal (marked by red boxes in Figure 3). Thirty-two intermolecular NOEs were identified in this section of the spectrum.

Assignment of the Intermolecular NOEs. The assignment of the cross-peaks in the difference spectrum to the specific pair wise interactions was carried out using the side-chain assignment of IFNα2 and IFNAR2 in their binary complex obtained in our previous study on the asymmetrically reverse-protonated complexes.[12] The docking model obtained previously[12] helped in the assignment procedure. Using these data, 90% of the cross-peaks identified as intermolecular NOEs, both in the aromatic and in the aliphatic regions of the double difference spectrum, were assigned. The full list of unambiguous distance restraints based on the assigned intermolecular NOE interactions is given in Table 1.

Modeling. Both IFNα2 and IFNAR2 undergo only limited conformational changes upon binding, and these changes occur mainly in the binding site regions.[17,19] Therefore, calculation of a docking model of the complex using the structures of the free proteins is possible. A new docking model of the IFNAR2/IFNα2 complex was calculated on the basis of the following data: (1) structures of the free complex components;[27,29] (2) NMR mapping of the respective binding sites;[17,19] (3) 97 intermolecular NOEs found in this study (Table 1, Supporting Information Table S1); (4) distance restraints previously obtained from double mutant cycle (DMC) analyses;[28] and (5) four intermolecular NOEs involving a single pair of residues found in our previous study.[19] The four intermolecular NOEs obtained in a previous study involved one of the amide protons of the complex components and therefore could not be observed in the present study. The docking was performed using the program HADDOCK,[24,37] which allows the input of experimental distance restraints to drive the docking calculation (see Experimental Methods). Violation analysis of the 200 final structures showed no NOE or DMC violations for all structures. The rmsd of the ensemble of the 10 best structures selected from the best cluster (ranked by the lowest HADDOCK score[24]) was 0.77 ± 0.12 Å for the backbone atoms and 1.08 ± 0.10 Å for all heavy atoms (Figure 4a, Table 2). The rmsd of the representative structure of the ensemble to our previous docking model of the IFNAR2/IFNα2 complex (calculated using the asymmetric reverse-protonation method[12]) is 1.16 Å for the backbone atoms and 1.28 Å for all heavy atoms. The distance restraints obtained in the present study are very well dispersed over the entire binding surface (Figure 4b), accounting for the high quality and accuracy of the new docking model of the complex. A full analysis of the docking model is shown in the Supporting Information (see Supporting Information Tables S2, S3). When only the 97 NOE constraints are used for the docking, only one cluster is obtained with a 0.6 Å rmsd of the ensemble of the 10 best structures (ranked by the lowest HADDOCK score[24]). The model of the complex obtained using only NOE data agrees very well with the conclusions on interacting residues from DMC and saturation transfer experiments.

DISCUSSION

In this Article, we present a powerful and straightforward double difference NOESY spectroscopy method that detects a very large number of intermolecular interactions among non-exchangeable protons in protein−protein complexes. Because of the high sensitivity of 2D NOESY spectra, this method can be widely applicable even for protein complexes well exceeding the 44 kDa molecular mass of the IFNα2/IFNAR2 complex. Previously developed procedures to study intermolecular interactions, such as 4D-isotope edited experiments or a combination of isotope-editing and isotope-filtering techniques,[11] suffer from significant losses in sensitivity for large protein complexes.

Table 2. Docking and Structural Statistics for the 10 Best IFNAR2/IFNα2 Model Structures[a]

	ensemble	representative structure
Docking Statistics		
HADDOCK score	−135.1 ± 4.7	−134.9
E_{vdw} [kcal/mol]	−93.4 ± 7.1	−101.3
E_{elec} [kcal/mol]	−493.5 ± 56.9	−428.4
E_{inter} [kcal/mol]	−371.2 ± 60.5	−318.2
E_{AIR} [kcal/mol]	215.7 ± 6.8	211.5
BSA [Å^2]	2753.1 ± 146.7	2756.8
rmsd from lowest energy structure [Å]	0.8 ± 0.1	0.7
cluster size	47	
number of AIR violations >0.3 Å	7.5 ± 0.5	8
number of NOE or DMC violations >0.3 Å	0	0
Structural Statistics		
rmsd backbone (heavy atom) [Å]	0.8 ± 0.1 (1.1 ± 0.1)	
rmsd all atoms at interface [Å]	1.3 ± 0.1	
rmsd backbone (heavy atom) from free IFNAR2 [Å]	1.0 ± 0.06 (1.1 ± 0.05)	0.9 (1.1)
rmsd backbone (heavy atom) from free IFNα2 [Å]	0.7 ± 0.04 (0.8 ± 0.05)	0.7 (0.8)
Deviations from Idealized Geometry		
rms deviation for bond angles [deg]	0.6	0.6
rms deviation for bond lengths [Å]	0.004	0.004
Ramachandran Analysis, Residues in:		
most favored regions [%]	78.1	78.3
additionally allowed regions [%]	20.2	20.6
generously allowed regions [%]	1.1	0.3
disallowed regions [%]	0.6	0.9

[a] Structure validation parameters were calculated using the PSVS − Protein Structure Validation Software suite.[34]

Because of the different physical basis for magnetization transfer (T_1 versus T_2 effects), our approach overcomes this sensitivity loss and, in principle, should be widely applicable to other biopolymeric complexes involving proteins overexpressed in *E. coli* (the vast majority of proteins studied by NMR and X-ray crystallography) and yeast cells.

The binding interface between IFNα2 and IFNAR2 consists of 30 IFNα2 and 30 IFNAR2 residues, and therefore the double difference NOESY spectrum is considerably less crowded than the NOESY spectra of the individual proteins of the complex. As a matter of fact, because the difference spectrum is free of intraresidue and intramolecular NOEs, it is much better resolved than the spectra of even very small proteins with the same number of residues as the binding interface of the complex. This considerably simplifies the assignment procedure.

In comparison with the asymmetric reverse-protonation method we developed recently, the double difference spectrum does not suffer from any artifacts due to incomplete exchange of amide protons or incomplete deuteration. All samples undergo the same procedure of preparation and solvent exchange in the double difference protocol, and, therefore, the degree of amide proton deuterium exchange should be sufficiently similar to cause the disappearance of practically all of the intramolecular H_N NOEs upon the double subtraction. Because no unlabeled amino acids were added to the growth medium, the intramolecular NOEs contributed by the residual protons that are incorporated in the proteins after expression in the 97% deuterated medium will involve pairs of such protons, and therefore the intensity (0.03 × 0.03 protonation) of these NOEs will be negligibly weak. The minor artifacts that do appear as a few lines of cross-peaks parallel to the diagonal in the aliphatic section of the double difference spectrum (Figure 3) do not hamper its analysis to any significant extent when the symmetry of the NOESY spectrum is taken into account.

The calculation of the double difference NOESY spectrum may appear to be complicated and subjective. In actuality, this is not the case, and the protocol that we describe in detail in the Experimental Methods should be fairly easy to implement using the standard 1D and 2D subtraction commands of the spectrometer software and a basic spectral analysis software such as NMRPipe.[21] The actual assignment of the intermolecular NOEs to specific protons is a major task and is the most time-consuming aspect of our protocol. However, assignment issues are a standard aspect of the NMR analysis of proteins and nucleic acids. The method developed by Yang and co-workers[1,38−40] has proven to be very powerful for side-chain proton assignment. In our case, the side-chain assignment was also facilitated by the high degree of similarity between the free and bound forms of the complex components, which allowed us to infer side-chain assignments of the bound proteins from their free form.[12] Because in many protein complexes the conformational changes upon binding involve only the binding site residues, it is possible to employ their overall structural similarity to obtain side-chain assignment in the bound state as we did in our previous work.[12]

In summary, we present here a novel method of detecting intermolecular NOEs in large protein complexes using a double difference NOESY spectrum. Our application of this technique to the 44 kDa IFNAR2/IFNα2 complex yielded nearly a 300%

increase in the number of intermolecular NOEs detected both in the aromatic and in the aliphatic regions of the spectrum as compared to the asymmetric labeling approach. These distance restraints enabled the calculation of a high-quality, accurate docking model of the IFNAR2/IFNα2 complex based only on NOE constraints. The very large number of experimental constraints imposed on the docking model should make it very close to the actual structure of the complex. We expect that the method described here could be very useful for other high molecular weight complexes due to its inherent sensitivity and ease of application. The crystal structure of the IFNAR2/IFNα2 complex is presently unknown. Therefore, the structure of the binding interface between the two molecules provided in this study sheds light on residue-specific interactions between two molecules that are of utmost biomedical importance.

■ ASSOCIATED CONTENT

Supporting Information. Figures describing in detail the way to apply the double difference NOESY methodology. Tables providing further information about the calculated docking model. This material is available free of charge via the Internet at http://pubs.acs.org.

■ AUTHOR INFORMATION

Corresponding Author
jacob.anglister@weizmann.ac.il

Present Addresses
[§]Laboratory of Cellular and Structural Biology, The Rockefeller University, New York, New York 10021, United States.
[||]Department of Biological Chemistry and Molecular Pharmacology, Harvard Medical School, Boston, Massachusetts 02115, United States.

■ ACKNOWLEDGMENT

This study was supported by the Israel Science Foundation and NIH Grant GM53329. J.A. is the Dr. Joseph and Ruth Owades Professor of Chemistry. We thank Professor Fred Naider for fruitful discussions and for help in editing the manuscript and Prof. Daiwen Yang (National University of Singapore) and Dr. Yingqi Xu (presently at Imperial College London) for their very valued assistance with implementation of their method for backbone and side-chain assignment to our system.

■ REFERENCES

(1) Xu, Y.; Zheng, Y.; Fan, J. S.; Yang, D. *Nat. Methods* **2006**, *3*, 931–937.
(2) Tugarinov, V.; Choy, W.-Y.; Orekhov, V. Y.; Kay, L. E. *Proc. Natl. Acad. Sci. U.S.A.* **2005**, *102*, 622–627.
(3) Otting, G.; Wüthrich, K. *Q. Rev. Biophys.* **1990**, *23*, 39–96.
(4) Otting, G.; Wüthrich, K. *J. Magn. Reson.* **1988**, *76*, 569–574.
(5) Ikura, M.; Bax, A. *J. Am. Chem. Soc.* **1992**, *114*, 2433–2440.
(6) Kogler, H.; Sörensen, O. W.; Bodenhausen, G.; Ernst, R. R. *J. Magn. Reson.* **1983**, *55*, 157–163.
(7) Breeze, A. L. *Prog. Nucl. Magn. Reson. Spectrosc.* **2000**, *36*, 323–372.
(8) Gross, J. D.; Moerke, N. J.; von der Haar, T.; Lugovskoy, A. A.; Sachs, A. B.; McCarthy, J. E.; Wagner, G. *Cell* **2003**, *115*, 739–750.
(9) Gross, J. D.; Gelev, V. M.; Wagner, G. *J. Biomol. NMR* **2003**, *25*, 235–242.
(10) Koglin, A.; Lohr, F.; Bernhard, F.; Rogov, V. V.; Frueh, D. P.; Strieter, E. R.; Mofid, M. R.; Guntert, P.; Wagner, G.; Walsh, C. T.; Marahiel, M. A.; Dötsch, V. *Nature* **2008**, *454*, 907–U968.
(11) Takeuchi, K.; Roehrl, M. H. A.; Sun, Z. Y. J.; Wagner, G. *Structure* **2007**, *15*, 587–597.
(12) Nudelman, I.; Akabayov, S. R.; Schnur, E.; Biron, Z.; Levy, R.; Xu, Y.; Yang, D.; Anglister, J. *Biochemistry* **2010**, *49*, 5117–5133.
(13) Fesik, S. W.; Zuiderweg, E. R. P. *J. Am. Chem. Soc.* **1989**, *111*, 5013–5015.
(14) Zvi, A.; Feigelson, D. J.; Hayek, Y.; Anglister, J. *Biochemistry* **1997**, *36*, 8619–8627.
(15) Zvi, A.; Kustanovich, I.; Hayek, Y.; Matsushita, S.; Anglister, J. *FEBS Lett.* **1995**, *368*, 267–270.
(16) Zvi, A.; Tugarinov, V.; Faiman, G. A.; Horovitz, A.; Anglister, J. *Eur. J. Biochem.* **2000**, *267*, 767–779.
(17) Chill, J. H.; Nivasch, R.; Levy, R.; Albeck, S.; Schreiber, G.; Anglister, J. *Biochemistry* **2002**, *41*, 3575–3585.
(18) Piehler, J.; Schreiber, G. *J. Mol. Biol.* **1999**, *289*, 57–67.
(19) Quadt-Akabayov, S. R.; Chill, J. H.; Levy, R.; Kessler, N.; Anglister, J. *Protein Sci.* **2006**, *15*, 2656–2668.
(20) Gasteiger, E.; Hoogland, C.; Gattiker, A.; Duvaud, S. e.; Wilkins, M. R.; Appel, R. D.; Bairoch, A. *Protein Identification and Analysis Tools on the ExPASy Server*; 2005; pp 571−607.
(21) Delaglio, F.; Grzesiek, S.; Vuister, G. W.; Zhu, G.; Pfeifer, J.; Bax, A. *J. Biomol. NMR* **1995**, *6*, 277–293.
(22) Johnson, B. A.; Blevins, R. A. *J. Biomol. NMR* **1994**, *4*, 603–614.
(23) Bax, A.; Ikura, M.; Kay, L. E.; Zhu, G. *J. Magn. Reson.* **1991**, *91*, 174–178.
(24) Dominguez, C.; Boelens, R.; Bonvin, A. M. J. J. *J. Am. Chem. Soc.* **2003**, *125*, 1731–1737.
(25) Brunger, A. T. *Nat. Protoc.* **2007**, *2*, 2728–2733.
(26) Brunger, A. T.; Adams, P. D.; Clore, G. M.; DeLano, W. L.; Gros, P.; Grosse-Kunstleve, R. W.; Jiang, J. S.; Kuszewski, J.; Nilges, M.; Pannu, N. S.; Read, R. J.; Rice, L. M.; Simonson, T.; Warren, G. L. *Acta Crystallogr., Sect. D: Biol. Crystallogr.* **1998**, *54*, 905–921.
(27) Chill, J. H.; Quadt, S. R.; Levy, R.; Schreiber, G.; Anglister, J. *Structure* **2003**, *11*, 791–802.
(28) Roisman, L. C.; Piehler, J.; Trosset, J. Y.; Scheraga, H. A.; Schreiber, G. *Proc. Natl. Acad. Sci. U.S.A.* **2001**, *98*, 13231–13236.
(29) Klaus, W.; Gsell, B.; Labhardt, A. M.; Wipf, B.; Senn, H. *J. Mol. Biol.* **1997**, *274*, 661–675.
(30) Hubbard, S. J.; Eisenmenger, F.; Thornton, J. M. *Protein Sci.* **1994**, *3*, 757–768.
(31) Hubbard, S. J.; Thornton, J. M.; Campbell, S. F. *Faraday Discuss.* **1992**, *93*, 13–23.
(32) Krissinel, E.; Henrick, K. *J. Mol. Biol.* **2007**, *372*, 774–797.
(33) Koradi, R.; Billeter, M.; Wüthrich, K. *J. Mol. Graphics* **1996**, *14*, 51−55, 29−32.
(34) Bhattacharya, A.; Tejero, R.; Montelione, G. T. *Proteins* **2007**, *66*, 778–795.
(35) DeLano, W. L. *Curr. Opin. Struct. Biol.* **2002**, *12*, 14–20.
(36) Meadows, D. H.; Jardetzky, O.; Epand, R. M.; Ruterjans, H. H.; Scheraga, H. A. *Proc. Natl. Acad. Sci. U.S.A.* **1968**, *60*, 766–772.
(37) de Vries, S. J.; van Dijk, M.; Bonvin, A. M. *Nat. Protoc.* **2010**, *5*, 883–897.
(38) Xu, Y.; Lin, Z.; Ho, C.; Yang, D. *J. Am. Chem. Soc.* **2005**, *127*, 11920–11921.
(39) Yang, D.; Zheng, Y.; Liu, D.; Wyss, D. F. *J. Am. Chem. Soc.* **2004**, *126*, 3710–3711.
(40) Zheng, Y.; Giovannelli, J. L.; Ho, N. T.; Ho, C.; Yang, D. *J. Biomol. NMR* **2004**, *30*, 423–429.